Proceedings of ICRC 2001: 2419 © Copernicus Gesellschaft 2001

ICRC 2001

γ-ray pulsars in the Gould Belt

C. A. Perrot and I. A. Grenier

Université Paris VII & CEA/Saclay, Service d'Astrophysique, 91191 Gif-sur-Yvette, France

Abstract. The dynamical evolution of the Gould Belt has been modelled in 3D and confronted to the spatial and velocity distributions of all HI and H_2 clouds within a few hundred parsecs from the Sun and to the Hipparcos distances of the nearby OB associations. The present-day data can be explained by the expansion of a shock wave, with an initial kinetic energy of $(1.0 \pm 0.1)\ 10^{52}$ erg, over a timespan of 26.4 ± 0.4 Myr, into the local interstellar medium and in the Galactic disc gravitational potential. The current Belt rim coincides with most of the nearby OB associations and H_2 clouds. Given the enhanced Belt supernova rate, pulsars born in the Belt in the last few million years are likely to account for persistent unidentified EGRET sources in the Belt. Simulations of the time evolution and visibility (for EGRET) of this pulsar population have been carried out. For standard pulsar emissivities and beaming fractions above 100 MeV, the resulting density map of pulsars visible above the Galactic diffuse emission shows that the asymmetric Belt signature across the sky is preserved over at least 5 Myr.

1 Introduction

The Gould Belt is a nearby starburst expanding disc where many collapsed stars such as pulsars must have formed in the past few million years. Sir John Herschel first pointed out in 1847 that the distribution of the brightest stars was asymmetric about the Galactic plane. The geometry of this young structure (most of the stars are less than 30-40 million years old) was then studied in 1874 by Benjamin A. Gould who determined its inclination and the direction of its poles. The Gould Belt also contains many interstellar clouds and Lindblad (1967) gave strong evidence for the Belt relation to the locally expanding HI gas. Famous H_2 complexes, such as Orion and Ophiuchus, are often mentioned in relation to the Belt, but no correlation study has been undertaken using all the nearby CO clouds. The flatness of the Belt and its tilt, some 20° to the Galactic plane, bears important information on the Belt origin, but remains very difficult to interpret. Various scenarii involve the oblique impact of a high-velocity cloud on the Galactic disc or a cascade of several supernova explosions (see Poppel (1997) for a review). Olano (2001) recently suggested that a supercloud was the common precursor of the Sirius supercluster, the Gould Belt and the Local Arm. The braking and compression of the supercloud while entering a spiral arm would have produced the Gould Belt and the Local Arm whereas the stellar cluster, unaffected by friction, would have moved on, out of the gas system.

In section 2, we will describe the dynamical model used to fit the current Belt geometry against the local CO and HI data and we will show its relation to the OB associations in the solar neighbourhood. In section 3 we will model the dynamical evolution of a population of γ-ray pulsars born within a few million years in the Belt to study their spatial distribution in the sky as seen by EGRET.

Correspondence to: C. Perrot (cperrot@cea.fr)

2 3D evolution model

The Gould Belt is well delineated both by the local group of early type stars and by a high concentration of HI and H_2 gas. Its evolution has been modelled in 3D (x, y, z in an inertial Galactic frame) and confronted to the spatial as well as velocity distributions of all HI and CO clouds within a few hundred parsecs from the Sun. To find the position and velocity centroid of the clouds, the longitude, latitude, and velocity data cubes of the relevant CO and HI surveys (Dame *et al.* (1987), Hartmann *et al.* (1996), and Strong *et al.* (1982)) were searched for local peaks of emission, i.e. cloud clumps, using the "clumpfind" tool developed by Williams *et al.* (1994). Various cuts in latitude and velocity were applied to keep all clouds within $\sim$ 600 pc from the Sun and to avoid contamination from background clouds in the Galactic disc or in the Local Arm. No attempt was made at cutting nearby clouds seen away from the characteristic Belt lane in l and b

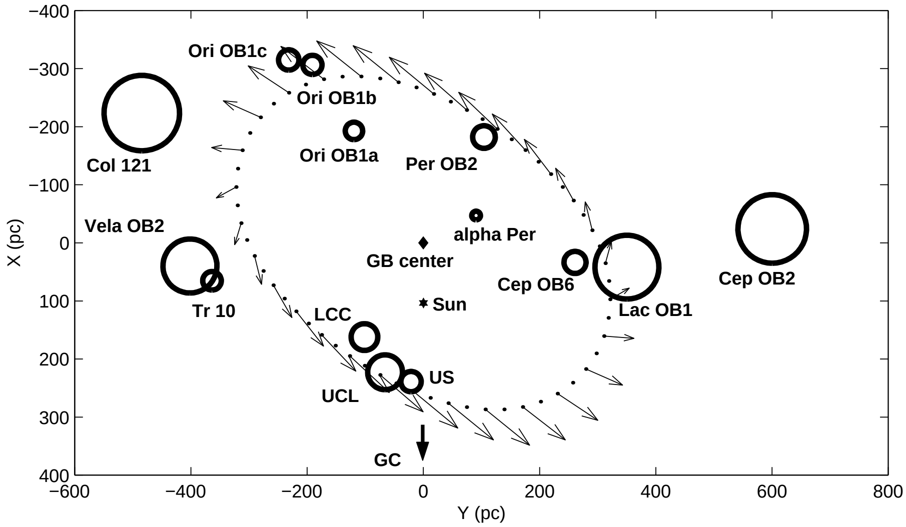

Fig. 1. Present position of the Gould Belt projected onto the Galactic Plane. The X-axis points to the Galactic Center, while the Y-axis points in the direction of the Galactic rotation. This non-inertial frame is centered on the Belt center. The velocity field in this frame outlines the current Belt expansion. The main nearby OB associations are plotted as thick-line circles using recent Hipparcos estimates of their distance and size.

since the Belt angular width is unknown. The resulting set of [l,b,v] coordinates of all selected clumps has then been confronted to the position and velocity of the modelled Belt using a maximum-likelihood test that allowed integration of the probability distributions along a given Belt and along the lines of sight of the observed clumps (Perrot & Grenier, in preparation). The likelihood function also included a distance probability for a subset of well-known clouds.

2.1 Basic assumptions

The model does not attempt to explain the origin of the outburst, but describes the lateral expansion of an inclined, cylindrical shock wave that sweeps momentum from the ambient interstellar medium. The height that best fits the data was found to be 60 ± 5 pc and was adopted hereinafter. As a consequence of the Galactic differential rotation, the circular section of the Belt rapidly evolves into an elliptical one. Additionally, the combined actions of the Galactic gravitational potential and of the interstellar density gradients further warp the Belt. So, we split it into 60 elementary pieces. Their contiguous surfaces delineated the Belt rim without any holes at each time step and allowed it to bend and warp easily because of the varying mass and velocity of the swept-up gas and under the gravitational pull of the Galactic disc.

The local gas distribution falls with height z above the Galactic plane as the combination of three Gaussian and one exponential:

$$\rho(z) = N_{1,\,HI}\ exp(-\frac{z^2}{2\sigma_1^2}) + N_{2,\,HI}\ exp(-\frac{z^2}{2{\sigma_2}^2})$$
$$+N_{3,\,HI}\ exp(-\frac{z}{\sigma_3}) + N_{H_2}\ exp(-\frac{z^2}{2{\sigma_{H_2}}^2})$$

with $N_{1,\,HI} = 0.395\ \mathrm{cm}^{-3}$, $\sigma_1 = 90.03$ pc, $N_{2,\,HI} = 0.107\ \mathrm{cm}^{-3}$, $\sigma_2 = 225.17$ pc, $N_{3,\,HI} = 0.064\ \mathrm{cm}^{-3}$, $\sigma_3 = 403.0$ pc, $N_{H_2} = 0.2\ \mathrm{cm}^{-3}$ and $\sigma_{H_2} = 74.0$ pc (Dickey & Lockman (1990), Dame *et al.* (1987)). A radial, galactocentric density gradient was also included which yielded equivalent results, so the sole z dependence on the interstellar density has been retained. In order to compute the interstellar gas momentum, we adopted for the Oort's constant and the Solar galactocentric radius the IAU recommended values namely $A_c = 14.5\ \mathrm{km.s^{-1}.kpc^{-1}}$ and $R_\odot = 8.5$ kpc. Finally, we calculated the torque induced by the gravitational potential of the local stellar mass density distribution, taken to have a volume density $\rho_* = 7.6\ 10^{-2}\ \mathrm{M_\odot.pc^{-3}}$ at z = 0 (Crezé *et al.*, 1998) and an exponential scale height $z_* = 260 \pm 60$ pc (Ojha *et al.*, 1996). We also assumed there was no internal pressure from supernova or stellar winds, and no external pressure from the interstellar medium. All the computations were done in an inertial Galactic reference frame in Cartesian coordinates. At $t = 0$, the Sun position was taken as ($x_\odot = -R_\odot$; $y_\odot = 0$; $z_\odot = 0$), the y-axis pointing in the direction of the Galactic rotation. The following parameters were used to describe the Belt and model its evolution: θ^i the initial direction of the Belt nodal line; ϕ^i the initial inclination of the Belt on the Galactic plane; l^i_{center} the initial galactic longitude of the center; d^i_{center} the initial distance of the center to the Sun; E_i the initial kinetic energy; τ the Belt age; H the Belt height (60 ± 5 pc). To reduce the number of free parameters, we assumed the center to be initially located at z = 0.

2.2 Results

The best fit yields characteristics for the present Gould Belt that are in good agreement with observations. In particular, conspicuous nearby H_2 complexes such as Perseus, Cepheus, Cassiopeia, and Lupus appear to be related to the Belt. As shown in Figure 1, the Belt also coincides with most of the nearby OB associations such as Per OB2, Ori OB1a & OB1c, LCC, UCL, US, Cep OB6, and Lac OB1, the positions of which are known from Hipparcos measurements (de Zeeuw *et al.* (1999)). The best fit yields a present inclination $\phi = 17.2° \pm 0.3°$ onto the Galactic plane, an age $\tau = 26.4 \pm$

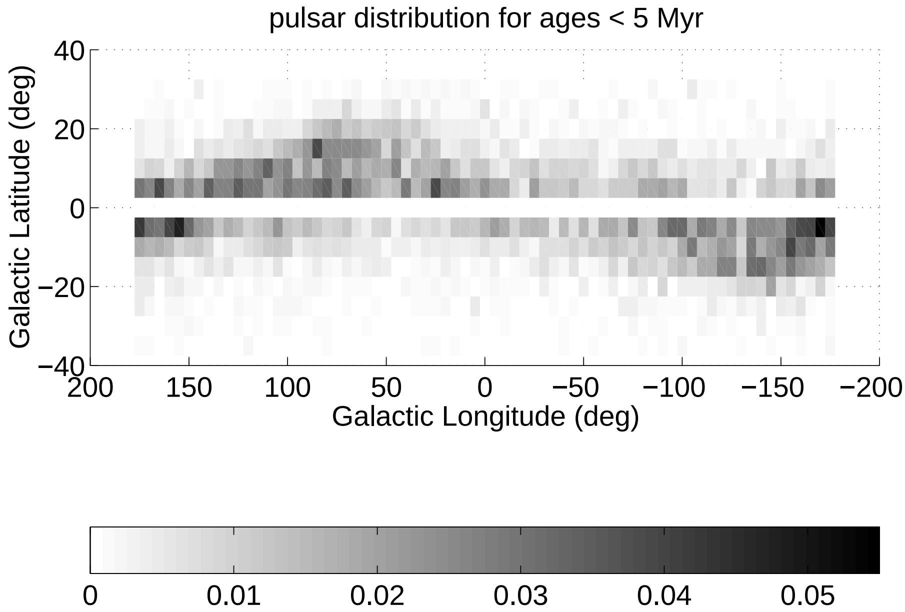

Fig. 2. Number density map at $|\ b\ |> 2.5°$ for pulsars born in the Gould Belt, with ages $0 < \tau < 5$ Myr. The visibility threshold is constructed from the interstellar γ-ray background from Hunter *et al.* (1997), the extragalactic background and the EGRET 4-year exposure map, following the 4 and 5 σ levels adopted in the 3rd EGRET catalogue

0.4 Myr and an initial energy $E_i = (1.0 \pm 0.1)\ 10^{52}$ erg. These values are comparable to those obtained by Moreno *et al.* (1999) in their modelling of the Belt versus the local stellar velocities and to the values obtained by Olano (1982) in his 2D modelling of the HI longitude-velocity distribution. The center of the Belt is located at a distance $d_{center}^{today} = 104 \pm 4$ pc from the Sun in the direction $l_{center}^{today} = 180° \pm 2°$. The final ellipse has a semi-major axis $a = 354 \pm 5$ pc and a semi-minor axis $b = 232 \pm 5$ pc. The resulting geometry appears to be independent of the presence or not in the fit of the complex of Taurus clouds, which are located near the Belt center.

A more realistic representation of the braking process has been introduced in the late stages of the Belt evolution as a drag force gradually applied to the Belt elements when their velocity falls into the 30 to 10 km/s interval. In parallel, each element becomes increasingly porous to the interstellar flow. The improvement in the fit is, however, very small and the resulting geometry is unchanged. The influence of an initial rotation of the Belt was also tested. It showed that the swept-up gas momentum clearly dominates the Belt dynamics.

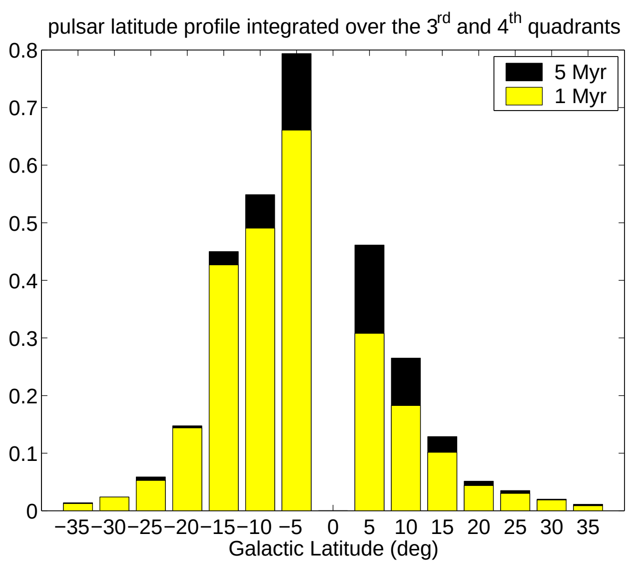

Fig. 3. Latitude profile of the number of visible pulsars integrated over negative longitudes for pulsar ages less than 1 and 5 Myr.

3 γ-ray pulsars in the Gould Belt ?

It has been suggested that pulsars born in the Gould Belt over the past few million years may account for persistent unidentified EGRET sources in the Belt (Grenier, 2000). The supernova rate in the Belt (20 to 27 SNe per Myr) is indeed 3 to 5 times larger than the local Galactic rate (5 to 10 SNe per Myr). Geminga is the first detected example of a Belt pulsar and, because of its proximity, the intrinsically faintest pulsar observed so far. It could, however, have been detected anywhere inside or in the vicinity of the Belt. Extrapolating from Geminga for half a decade in spin-down luminosity, to $\dot{E} = 10^{33}$ erg/s $\Longrightarrow L_{>100MeV} \sim 6\ 10^{32}$ erg/s over 1 sr, suggests that a pulsar 10 times as old as Geminga, i.e. 3-Myr old, remains easily visible throughout the Belt. Ten times fainter emission from this old pulsar seen at grazing angles would remain visible to 350 pc. Harding & Zhang (2001) showed that off-beam γ-ray pulsars could indeed explain nearby EGRET sources. These pulsars would be viewed at a large angle to the neutron star magnetic pole, in a configuration where the line of sight misses both the bright γ-ray and radio beams. Within the framework of the polar-cap model described by Daugherty & Harding (1996), a synchrotron-pair cascade at low altitude produces the hard on-beam emission whereas primary electrons at a higher altitude produce a wider and softer off-beam of γ-rays through curvature radiation. Such off-beam pulsars being $\sim$4 times more numerous than the on-beam ones would be particularly suitable to explain EGRET sources in the Belt because of the soft spectrum and low luminosity characterizing this population of unidentified sources (Grenier, 2000).

3.1 Simulation

We investigated the dynamical evolution of a population of pulsars born in the expanding Belt with large kick velocities typical of radio pulsars. Pulsars were generated at random at a constant rate within a few million years, and uniformly in a thick torus inside the Belt rim (as situated at the time of the pulsar birth). Radially, the torus covers the outer half of the elliptical Belt disc and perpendicular to the Belt plane, it is limited to ± 20 pc in height. The pulsar initial velocity results from the combination of the local Galactic rotation velocity and a random component following a Maxwellian distribution with dispersion $\sigma_v = \sqrt{3} \times 300$ km/s, i.e. a mean of 480 km/s (Lorimer *et al.*, 1997). The integration of motion was done in the Galactic gravitational potential given by Paczynski (1990). The following standard parameters for the γ-ray pulsed emission were assumed: a luminosity $L_{>100MeV} = 1.5\ 10^{16} \times \dot{E}_{spindown}^{1/2}$ erg/s over 1 sr (Thompson *et al.*, 1997); a $\boldsymbol{B}$ field following a Gaussian distribution in $log\,(B)$with a mean of 12.4 and dispersion of 0.3; an initial spin period $P_0 = 30$ ms and a period at time t given by $P(t) = [P_0^2 + \frac{16\pi^2 R_{NS}^6 B^2}{3Ic^3}]^{1/2}$; a neutron star radius $R_{NS} = 10^6$ cm and moment of inertia I = 10^{45} g cm^2; a period derivative given by $P\dot{P} = \frac{8\pi^2 R_{NS}^6 B^2}{3Ic^3}$; a random magnetic inclination α and aspect angle ζ; a beam opening angle $\theta \simeq 10\ \theta_{polar\ cap}$; a birth rate of 25 Myr^{-1} in the Belt.

3.2 Results

Figure 2 shows the number density map, in $5° \times 5°$ bins at $\mid b \mid > 2.5°$, obtained for pulsars born in the Gould Belt with an age < 5 Myr and visible by EGRET. To account for the non-uniform sensitivity of EGRET across the sky, the visibility threshold was constructed using the interstellar γ-ray background from Hunter *et al.* (1997) and the 4-year exposure (P1234) of the EGRET survey (Hartman *et al.*, 1999). Detection thresholds of 4 and 5 σ above the interstellar and extragalactic background were adopted as in the 3rd EGRET catalogue (Hartman *et al.*, 1999). As one can see, the Belt signature is well preserved over at least 5 Myr against the rapid pulsar migration and the Belt geometrical evolution. The north-south asymmetry about the Galactic plane in the 1st+2nd or in the 3rd+4th quadrants corresponds to a 2:1 ratio in the total number of visible objects in these areas. The latitude profiles integrated over the 3rd+4th quadrants in Figure 3 show that this contrast is little reduced from 1 to 5 Myr. So, the Belt signature should be preserved beyond 5 Myr.

4 Conclusion

The Gould Belt time evolution has been modelled in 3D and fitted against the (l,b) position and velocity of the CO and HI clouds of the solar neighbourhood. The position derived for the Belt is found to coincide with the main nearby OB associations and molecular clouds. The initial kinetic energy of $E_i = (1.0 \pm 0.1)\ 10^{52}$ erg amounts to that of 10 supernovae, as previously estimated by Olano (1982). The dynamical age of 26 ± 0.4 Myr found for the Belt is significantly younger than the nuclear age of 30 to 40 Myr derived from the lifetime of the Belt stars. This discrepancy was also noted in previous models fitted against the HI or the stellar velocity fields (Olano (1982), Moreno *et al.* (1999)). One way to get an older structure is to let it cross the Galactic plane in its see-saw motion in the Galactic potential before reaching its current position. Such a solution to the fit has been found and is currently investigated.

The Belt dynamical model has been used to investigate the possible contribution of off-beam γ-ray pulsars to the unidentified EGRET sources in the Belt. As a first step, a density map of visible pulsars has been constructed for ”reasonable” emission parameters which shows that the characteristic spatial signature of the Belt is preserved over at least 5 Myr despite the geometrical evolution of the Belt, its large apparent angular width, and the rapid migration of pulsars from their birth location. We now intend to use this model to constrain the pulsar emission parameters, such as the beam opening angle, intensity and spectral index, required to match the characteristics of the EGRET source population.

References

Crezé, M. *et al.*, A&A, **329**, 920-936, 1998.
Dame, T. M. *et al.*, ApJ, **322**, 706, 1987.
Daugherty, J. K., & Harding A. K., ApJ, **458**, 278, 1996.
Dickey, J. M., & Lockman, F. J., ARA&A, **28**, 215, 1990.
Grenier, I. A., A&A, **364**, L93, 2000.
Harding, A. K., & Zhang, B., ApJ, **548**, L37, 2001.
Hartman, R. C. *et al.*, A&AS, **123**, 179, 1999.
Hartmann, D. *et al.*, A&AS, **119**, 115, 1996.
Hunter, S. D. *et al.*, ApJ, **481**, 205, 1997.
Lindblad, P. O., Bulletin of the Astronomical Institute of the Netherlands, **19**, 34, 1967.
Lorimer, D. R. *et al.*, MNRAS, **289**, 592, 1997.
Moreno, E. *et al.*, ApJ, **522**, 276, 1999.
Ojha, D. K. *et al.*, A&A, **311**, 456, 1996.
Olano, C. A., A&A, **112**, 195, 1982.
Olano, C. A., AJ, **121**, 295, 2001.
Paczynski, B., ApJ, **348**, 485, 1990.
Poppel, W. G. L., Fundamentals of Cosmic Physics, **18**, 1, 1997.
Strong, A. W. *et al.*, MNRAS, **201**, 495, 1982.
Thompson, D. J. *et al.*, Proc. of the 4th Compton Symposium, Editors C. Dermer, M. Strickman, & J. Kurfess, Williamsburg, VA, AIP, **410**, 39, 1997.
Williams, J. P. *et al.*, ApJ, **428**, 693, 1994.
de Zeeuw, P. T. *et al.*, ApJ, **117**, 354, 1999.